Direct Observation of Guanine Radical Cation Deprotonation in G-Quadruplex DNA

ARTICLE *in* JOURNAL OF THE AMERICAN CHEMICAL SOCIETY · DECEMBER 2014

Impact Factor: 12.11 · DOI: 10.1021/ja510285t · Source: PubMed

5 AUTHORS, INCLUDING:

Kunhui Liu
Beijing Normal University
20 PUBLICATIONS **72** CITATIONS
SEE PROFILE

Jie Jialong
Chinese Academy of Sciences
2 PUBLICATIONS **3** CITATIONS
SEE PROFILE

Di Song
Chinese Academy of Sciences
29 PUBLICATIONS **192** CITATIONS
SEE PROFILE

JACS
JOURNAL OF THE AMERICAN CHEMICAL SOCIETY

Article

pubs.acs.org/JACS

Direct Observation of Guanine Radical Cation Deprotonation in G-Quadruplex DNA

Lidan Wu,‡ Kunhui Liu,‡ Jialong Jie, Di Song, and Hongmei Su*

Beijing National Laboratory for Molecular Sciences (BNLMS), Institute of Chemistry, Chinese Academy of Sciences, Beijing 100190, China

Supporting Information

ABSTRACT: Although numerous studies have been devoted to the charge transfer through double-stranded DNA (dsDNA), one of the major problems that hinder their potential applications in molecular electronics is the fast deprotonation of guanine cation ($G^{+\bullet}$) to form a neutral radical that can cause the termination of hole transfer. It is thus of critical importance to explore other DNA structures, among which G-quadruplexes are an emerging topic. By nanosecond laser flash photolysis, we report here the direct observation and findings of the unusual deprotonation behavior (loss of amino proton N_2−H instead of imino proton N_1−H) and slower (1−2 orders of magnitude) deprotonation rate of $G^{+\bullet}$ within G-quadruplexes, compared to the case in the free base dG or dsDNA. Four G-quadruplexes $AG_3(T_2AG_3)_3$, $(G_4T_4G_4)2$, $(TG_4T)4$, and $G_2T_2G_2TGTG_2T_2G_2$ (TBA) are measured systematically to examine the relationship of deprotonation with the hydrogen-bonding surroundings. Combined with in depth kinetic isotope experiments and pK_a analysis, mechanistic insights have been further achieved, showing that it should be the non-hydrogen-bonded free proton to be released during deprotonation in G-quadruplexes, which is the N_2−H exposed to solvent for G bases in G-quartets or the free N_1−H for G base in the loop. The slower N_2−H deprotonation rate can thus ensure less interruption of the hole transfer. The unique deprotonation features observed here for G-quadruplexes open possibilities for their interesting applications as molecular electronic devices, while the elucidated mechanisms can provide illuminations for the rational design of G-quadruplex structures toward such applications and enrich the fundamental understandings of DNA radical chemistry.

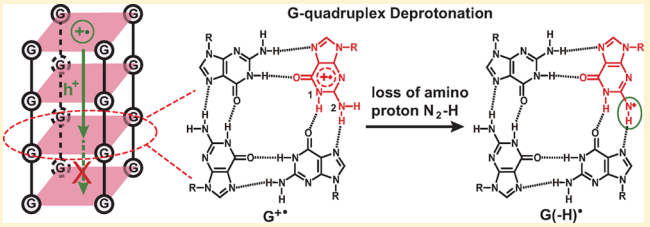

INTRODUCTION

The charge transfer through deoxyribonucleic acid (DNA) strands has attracted considerable attention during the past few decades due to its biological importance[1] and potential applications in molecular electronics.[2,3] Especially, a large number of studies[4−8] have been carried out on hole transfer in double-stranded DNA (dsDNA) which is believed to be a promising candidate for developing electronic devices.[9−11] As is well-known, guanine (G) has the lowest oxidation potential among the four DNA bases and is the most readily oxidized base.[12,13] Therefore, for the hole transfer in DNA, the injected hole is always trapped in guanine, and the migration of hole in DNA is consequently a short distance charge-transfer process between stacked guanine bases.[14−16] During the process, the deprotonation of guanine cation radical ($G^{+\bullet}$) to form neutral radical ($G-H^{\bullet}$) is considered to be the most critical reaction in competition with hole transfer in DNA.[17−19] Due to the fast deprotonation of $G^{+\bullet}$ in dsDNA (with a rate constant of 10^6 to 10^7 s^{-1}),[17,18] the distance of dsDNA-mediated hole transfer is limited to be slightly >200 Å.[5,6] To overcome this limit that has hindered hole transfer over longer distance, which has been key to the application of DNA molecules in molecular electronic devices for decades, it is of critical importance to explore other DNA structures with efficient conductivity and slower deprotonation rate.

G-quadruplexes are an emerging topic for developing DNA-based molecular electronic devices because of their unique hole-trapping property and their high conductance.[20−25] These advantages are due to the highly ordered DNA structures arising from the self-assembly of particular G-rich DNA sequences.[26] The unique structure of G-quadruplex consists of stacked G-quartets where each G-quartet, as shown in Scheme 1, is a planar array of four Hoogsteen-bonded guanines,

Scheme 1. Model Structure of G-Quartet and GC Base Pair

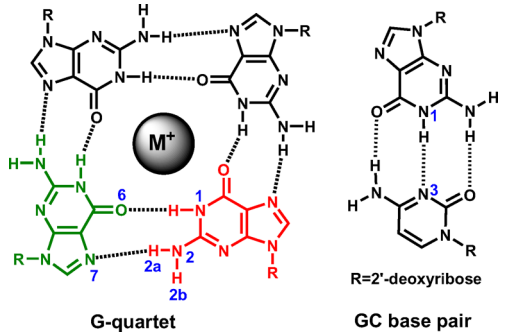

Received: October 7, 2014
Published: December 15, 2014

DOI: 10.1021/ja510285t
J. Am. Chem. Soc. 2015, 137, 259−266

stabilized by metal cations that serve to screen electrostatic repulsion between the negatively charged phosphate groups of the backbone.[27] The question arises that whether G-quadruplex can be a better candidate as conducting molecular wire. When assessing the charge transfer efficiency along the novel G-quadruplex structure, deprotonation rate is an important parameter due to the competition between $G^{+\bullet}$ deprotonation and hole transfer.[17] If the deprotonation rate in G-quadruplex is slower than that in dsDNA, the hole transfer could be less interrupted, and the hole transfer efficiency could be improved.

According to previous studies,[17,28] the deprotonation rate constant is related to the deprotonation site. In the free G base after one-electron oxidation, $G^{+\bullet}$ is known to deprotonate the imino proton (N_1–H) to generate $G(N_1\text{–H})^{\bullet}$ (eq 1) with the

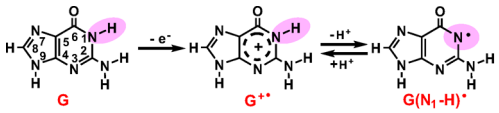

[1]

rate constant of 1.8×10^7 s^{-1} at pH 7.0,[17] due to the more acidic nature of N_1–H (pK_a = 3.9) compared to the amino proton N_2–H (pK_a = 4.7).[29] For 1-methylguanine (mG), of which N_1–H is substituted by methyl group and thus only the amino proton (N_2–H) loss could possibly occur, the one-electron oxidation is followed by N_2–H deprotonation to form $mG(N_2\text{–H})^{\bullet}$ (eq 2) with the rate constant of 3.5×10^5 s^{-1} at

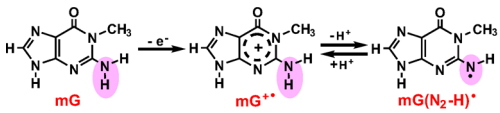

[2]

pH 7.1.[28] In dsDNA, the G base is paired with cytosine (C) through hydrogen bonding (Scheme 1), where the effect of base pairing is to transfer the N_1 proton of $G^{+\bullet}$ to N_3 of C in the base pair, as the protonation pK_a of N_3 in C (4.3) is slightly higher than the deprotonation pK_a of N_1 in $G^{+\bullet}$ (3.9).[17,18] The N_1–H deprotonation occurs along the central hydrogen bond in dsDNA, and then the proton is eventually released into solvent.[17,18] In the G-quadruplex, the imino and amino protons have more complicated surroundings, where each G base is hydrogen bonded to another two G bases to form G-quartet. Depending on which proton (N_2–H or N_1–H) is to be released, the deprotonation rate constant in G-quadruplex surrounding might be quite different from those in free G base and duplex DNA.

Herein, we are motivated to investigate the deprotonation process in G-quadruplexes, which remains elusive to a large extent in past studies. Using the highly potent $SO_4^{-\bullet}$ radical to oxidize G-quadruplex, the $G^{+\bullet}$ (hole) is produced, and its subsequent deprotonation is directly monitored by nanosecond laser flash photolysis. Unusual deprotonation behavior (loss of amino proton N_2–H instead of imino proton N_1–H) and slower (1–2 orders of magnitude) deprotonation rate of $G^{+\bullet}$ within G-quadruplexes are observed, which are distinct from the case in the free base dG or dsDNA. Four G-quadruplexes are measured systematically to examine the relationship of deprotonation with G base surroundings. By further kinetic isotope effect (KIE) experiment and pK_a analysis, the deprotonation mechanisms in G-quadruplexes are elucidated. The results suggest that G-quadruplex can be a more promising structure than dsDNA to apply in molecular electronic devices in terms of the slower deprotonation rate that could result in less interruption and longer distance of charge transfer. Also importantly, the mechanistic insights obtained here can provide guidance for rational design of G-quadruplex structure toward such applications.

MATERIALS AND METHODS

Materials. The DNA oligonucleotides $AG_3(T_2AG_3)_3$, $G_4T_4G_4$, TG_4T, and $G_2T_2G_2TGTG_2T_2G_2$ (TBA) were purchased from SBS Genetech Co., Ltd. (China) in the PAGE-purified form. Single-strand concentrations were determined by monitoring the absorbance at 260 nm in the UV–vis spectra and using the corresponding extinction coefficients of 228500, 115200, 57800, and 143300 M^{-1} cm^{-1} for $AG_3(T_2AG_3)_3$, $G_4T_4G_4$, TG_4T, and TBA, respectively.[30] The G-quadruplexes were prepared as follows: The oligonucleotide samples were dissolved in 50 mM potassium phosphate buffer solution for $(TG_4T)4$ and TBA or in 50 mM sodium phosphate buffer solution for $AG_3(T_2AG_3)_3$ and $(G_4T_4G_4)2$ at pH 7.0. The mixture was then heated to 90 °C for 10 min, cooled down to room temperature with a cooling rate of 0.5 °C/min, and then incubated at 4 °C for 12 h. The dsDNA was formed using $AG_3(T_2AG_3)_3$ and its complementary strand. Equal moles of $AG_3(T_2AG_3)_3$ and its complementary sequence were dissolved in 50 mM potassium phosphate buffer (pH 7.0). The annealing process was the same as forming quadruplex. The formation of quadruplexes was confirmed by circular dichroism (CD) spectroscopy and the duplex formation was confirmed by the fluorescence of ethdiium bromide (EB). Deoxy-guanosine (dG) was purchased from TCI. Potassium persulfate, sodium persulfate, and EB were purchased from Sigma. The potassium phosphate buffer and sodium phosphate buffer in H_2O or D_2O were purchased from Beijing Solarbio Science & Technology Co., Ltd. All the reagents were used as received.

CD Spectroscopy. CD experiments were performed at room temperature using a Jasco-815 spectropolarimeter. Each measurement was recorded from 200 to 320 nm in a 1 cm path length quartz cuvette at a scanning rate of 100 nm/min. The final data were the average of three measurements. The concentration of G-quadruplex DNA is 20 μM. The scan of the buffer alone was used as the background, which was subtracted from the average scan for each sample.

Laser Flash Photolysis. Nanosecond time-resolved transient absorption spectra were measured using a nanosecond flash photolysis setup Edinburgh LP920 spectrometer (Edinburgh Instruments Ltd.), combined with a Nd:YAG laser (Surelite II, Continuum Inc.). The sample was excited by a 355 nm laser pulse (1 Hz, 10 mJ/pulse, fwhm ≈ 7 ns). The analyzing light was from a 450W pulsed xenon lamp. A monochromator equipped with a photomultiplier for collecting the spectral range from 300 to 700 nm was used to analyze transient absorption spectra. Data were analyzed by the online software of the LP920 spectrophotometer.

Generation of Sulfate Radical Anions. Sulfate radicals, $SO_4^{-\bullet}$, were generated by the photodissociation of peroxodisulfate anions ($S_2O_8^{2-}$) by nanosecond 355 nm laser pulses (eq 3). Depending on the buffer used (Na^+ or K^+), the $Na_2S_2O_8$ or $K_2S_2O_8$ is photolyzed as the $SO_4^{-\bullet}$ precursor.

$$S_2O_8^{2-} \xrightarrow{h\nu} 2SO_4^{-\bullet} \quad (3)$$

The sulfate radical $SO_4^{-\bullet}$ has transient absorption (Figure S1) with the resolved band at 440 nm and a shoulder at 330 nm, which is in good agreement with the spectra reported previously.[19] The photodissociation of $S_2O_8^{2-}$ is rapid, and all $SO_4^{-\bullet}$ are generated within the ~14 ns laser pulse duration.[19] As a result, the formation dynamics of $SO_4^{-\bullet}$ does not interfere with the detection for the $SO_4^{-\bullet}$ + G reaction. The concentration of $SO_4^{-\bullet}$ can be estimated by the absorbance at 450 nm using an extinction coefficient of 1600 M^{-1} cm^{-1},[31] which is 1.9 μM and much smaller than the concentration of G-quadruplex (at least 30 μM). With the G-quadruplex in large excess, the bimolecular reaction of $SO_4^{-\bullet}$ oxidizing G-quadruplex becomes a pseudo first-order reaction. It is also expected that only one G base may be oxidized by $SO_4^{-\bullet}$, yielding one electron loss center in the G-quadruplex initially.

DOI: 10.1021/ja510285t
J. Am. Chem. Soc. 2015, 137, 259–266

RESULTS AND DISCUSSIONS

Structural Characterization of G-Quadruplex DNAs. In the presence of K^+ or Na^+, the four G-rich DNA sequences can form the well-established G-quadruplex structures,[32−37] respectively, which are confirmed by CD spectra (see Figure S2). Schematic description of the four G-quadruplex DNAs are shown in Scheme 2. The single human telomere sequence $AG_3(T_2AG_3)_3$ folds into an antiparallel basket-type G-quadruplex DNA with two lateral loops and a central diagonal loop in the presence of Na^+.[32,33] For Oxytricha telomere repeat sequences $G_4T_4G_4$, the dimer-hairpin-folded antiparallel G-quadruplex structure is formed in the Na^+ buffer solution.[34,35] Tetramolecular TG_4T will assemble to form a stable parallel G-quadruplex DNA in the presence of K^+.[35,36] In the case of TBA, an antiparallel chair-type G-quadruplex including two T-T lateral loops and a T-G-T lateral loop is formed by the single TBA sequence in the presence of K^+.[23,37]

Scheme 2. Schematic Structural Diagrams For the G-Quadruplex DNA[a] of $AG_3(T_2AG_3)_3$ (a), $(G_4T_4G_4)2$ (b), $(TG_4T)4$ (c), and TBA (d)

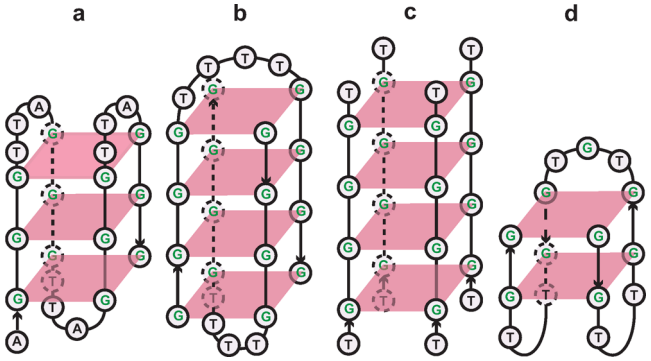

[a]Arrows denote 5′-3′ strand alignment for each DNA. The stabilizing metal ions (K^+ or Na^+) between the two G-quartets are omitted.

Oxidation and Deprotonation of G-Quadruplexes $AG_3(T_2AG_3)_3$, $(G_4T_4G_4)2$, and $(TG_4T)4$. In the G-quadruplex, all nucleobases are subject to oxidation by the instantaneously generated $SO_4^{-\bullet}$. However, the subsequent hole transfer from the initially formed electron loss centers to G site will occur and complete within 50 ns[17] due to the lowest oxidation potential of G among the four DNA bases.[12,13] As a result, it is the G base in G-quadruplex that is eventually oxidized by $SO_4^{-\bullet}$. To assist in understanding the deprotonation process in G-quadruplex, the one-electron oxidation of the free base dG by $SO_4^{-\bullet}$ under laser flash photolysis is first examined as a reference (Figure 1A). It is well-known that guanine cation radical $G^{+\bullet}$ is produced and then deprotonates to generate $G(N_1-H)^\bullet$ radical by the rapid loss of imino proton at pH 7.0 (eq 1),[17,29] with the oxidation and deprotonation rate constants of 7.2×10^9 M^{-1} s^{-1} and 1.8×10^7 s^{-1}, respectively.[17] In the current experiment with 3 mM concentration of dG, the oxidation and deprotonation completed within ~100 ns. The neutral radical $G(N_1-H)^\bullet$ is the only transient species absorbing at μs time scale as shown in Figure 1A. The standard transient spectra for $G(N_1-H)^\bullet$ radical can thus be obtained, which is featured with two resolved bands at 380 and 500 nm as well as flat absorption above 600 nm.[19,28,29]

Similar laser flash photolysis experiments were performed for the oxidation of G-quadruplex DNA by $SO_4^{-\bullet}$. In the transient

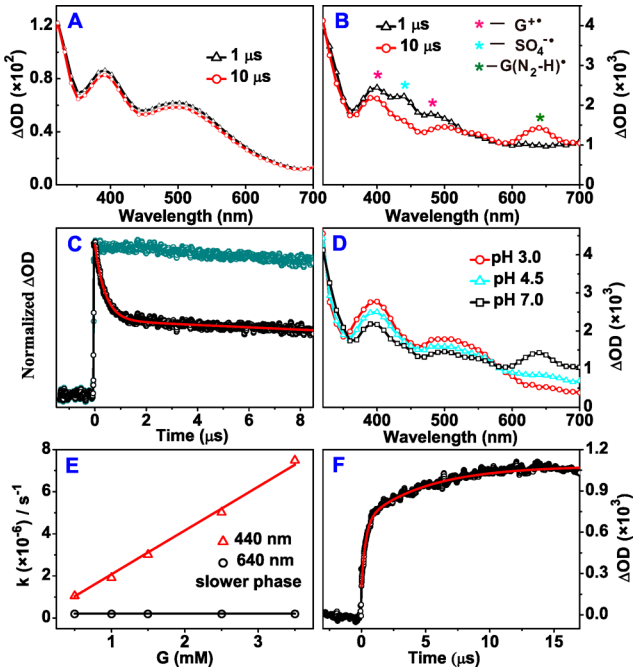

Figure 1. Transient UV−vis spectra for buffer solution (pH = 7.0) of (A) dG (3 mM) + $Na_2S_2O_8$ (120 mM). (B) G-quadruplex $AG_3(T_2AG_3)_3$ ([G] = 1.5 mM) + $Na_2S_2O_8$ (120 mM) upon 355 nm laser flash photolysis. (C) Kinetics trace at 440 nm after excitation of $Na_2S_2O_8$ (120 mM) solution in the absence (green circle) or presence (black circle) of G-quadruplex $AG_3(T_2AG_3)_3$ ([G] = 1.5 mM), with the single-exponential fit to the data (red solid line). (D) Transient UV−vis spectra at 10 μs after excitation of (B) solution at pH 3.0 (red circle), 4.5 (blue triangle), and 7.0 (black square). (E) Concentration dependence for the rate constants obtained from the fast decay of 440 nm band (red triangle) and the slower phase increase of 640 nm band (black circle), respectively. (F) Kinetics trace at 640 nm after excitation of (B) solution, with the double-exponential fits to the data (solid line).

spectra obtained for the mixed solution of G-quadruplex $AG_3(T_2AG_3)_3$ and $Na_2S_2O_8$ at pH 7.0 after 355 nm laser excitation (Figure 1B), two peaks at 400 and 440 nm, and a broad band around 480 nm are exhibited at the early time (1 μs). As the reaction proceeds with time, the absorbance at 400, 440, and 480 nm decays and a new peak at 640 nm builds up in the 10 μs spectra (Figure 1B). These signals are originated from $SO_4^{-\bullet}$ oxidizing G-quadruplex and its subsequent reactions. The 355 nm photolysis of the G-quadruplex alone does not generate any signal.

The band at 440 nm observed in the 1 μs spectra is most probably arising from $SO_4^{-\bullet}$ since $SO_4^{-\bullet}$ has characteristic absorption centered at 440 nm (see Figure S1). The oxidation rate of G-quadruplex by $SO_4^{-\bullet}$ can thus be measured by following the decay of 440 nm band. As shown in Figure 1C, the self-decay of $SO_4^{-\bullet}$ at 440 nm is quite slow. Markedly, the 440 nm decay is accelerated in the presence of G-quadruplex $AG_3(T_2AG_3)_3$ (Figure 1C), due to the efficient chemical quenching of $SO_4^{-\bullet}$ via reacting with the G-quadruplex. After the fast decay, the intensity at 440 nm almost keeps constant in the next few microseconds, demonstrating that the residual absorbance at 440 nm is attributed to a long-lifetime species, i.e., the deprotonated neutral radical that has absorption at 440 nm[17,28,29] and decays in ms time scale.[38] Further, the concentration dependence of the kinetics at 440 nm is assessed through changing the G-quadruplex concentration from 0.5 to

DOI: 10.1021/ja510285t
J. Am. Chem. Soc. 2015, 137, 259−266

3.5 mM (As the reaction site within G-quadruplex is actually G bases, the concentration of G-quadruplex is denoted by the concentration of G base). As shown in Figure 1E, the 440 nm decay rate constant increases as the concentration of G-quadruplex $AG_3(T_2AG_3)_3$ increases with linear dependence, which further indicates that the fast decay component at 440 nm is due to the bimolecular reaction of $SO_4^{-\bullet}$ with G-quadruplex $AG_3(T_2AG_3)_3$. From the slope, the second-order rate constant k_O for the oxidation is deduced to be 2.1×10^9 M^{-1} s^{-1}. It shows here that the oxidation rate constant of G-quadruplex $AG_3(T_2AG_3)_3$ by $SO_4^{-\bullet}$ is smaller than that of free base dG (7.2×10^9 M^{-1} s^{-1}).[17] This explains why the $SO_4^{-\bullet}$ band at 440 nm and its decay process can be observed for the G-quadruplex (Figure 1B), but not for the free base dG (Figure 1A).

Another difference between G-quadruplex and dG is the deprotonation process of $G^{+\bullet}$ formed after oxidation, which appears to be slower in G-quadruplex than that of dG. As a result, the characteristic absorption bands at 400 and 480 nm consistent with the $G^{+\bullet}$ spectral feature[17,29] are observed in the 1 μs spectra as shown in Figure 1B. In the case of free base dG, $G^{+\bullet}$ is subject to fast deprotonation (1.8×10^7 s^{-1})[17] to produce $G(N_1-H)^\bullet$ within 100 ns, so the transients at 1 μs are solely due to $G(N_1-H)^\bullet$ without $G^{+\bullet}$ (Figure 1A). The slower deprotonation rate in G-quadruplex may be caused by the different deprotonation behavior as discussed below.

As shown in Figure 1B (10 μs spectrum), the decay of the $G^{+\bullet}$ bands at 400 and 480 nm is accompanied by the buildup of a new peak at 640 nm with the same time scale (~6 μs half rise time as shown in Figure S3). This indicates that the new peak at 640 nm may correspond to the $G^{+\bullet}$ decay product. In neutral solution, the dominant process accounting for $G^{+\bullet}$ decay is the fast deprotonation.[19] It shows further in the control experiment that the transient absorbance around 640 nm increases with the increase of pH (Figure 1D). At pH 3.0 when $G^{+\bullet}$ deprotonation can not occur, there is no considerable absorption around 640 nm, while this band intensity is significantly enhanced at pH 7.0. The pH dependence demonstrates that the buildup of the 640 nm band is attributed to the $G^{+\bullet}$ deprotonation to form the neutral radical. The deprotonation may lead to two neutral radicals, $G(N_1-H)^\bullet$ or $G(N_2-H)^\bullet$, depending on which proton (imino or amino) is to be released. Considering that $G(N_1-H)^\bullet$ only has flat absorption (no absorption peak) above 600 nm,[19,28,29] the peak at 640 nm is most likely ascribed to another neutral G radical, the N_2-H deprotonated radical $G(N_2-H)^\bullet$, which is featured by absorption peak around 620 nm.[39,40] The 620 nm absorption peak has been regarded to be specific for $G(N_2-H)^\bullet$ and used to distinguish from $G(N_1-H)^\bullet$.[39,40] In this case, it indicates that after one-electron oxidation, the deprotonation site in G-quadruplex occurs at the amino group (N_2-H), which is different from the imino deprotonation (N_1-H) in the free base dG.

According to previous studies, the N_1-H deprotonation rate constant (1.8×10^7 s^{-1})[17] of $G^{+\bullet}$ is larger than N_2-H (3.5×10^5 s^{-1}),[28] which suggests that the deprotonation rate constant in G-quadruplexes can further assist in distinguishing the deprotonation site. We monitored the kinetics of the 640 nm band due to the $G^{+\bullet}$ deprotonation. As shown in Figure 1F, the transients at 640 nm involve a fast increasing process and a slow one, which can be well fitted by biexponential function with time constants of 332 and 4925 ns, respectively. The fast time constant (332 ns) is consistent with the bimolecular oxidation rate (320 ns) obtained from the fast decay of 440 nm (Figure 1C) and also exhibits linear dependence on the concentration of G-quadruplex (data not shown, which is almost identical to the 440 nm concentration dependence shown in Figure 1E), indicating that the fast component results from the bimolecular oxidation reaction to form $G^{+\bullet}$. In contrast, as shown in Figure 1E, the rate constants of the 640 nm slower phase are observed to be independent of G-quadruplex concentration. This implies that the 640 nm slower phase corresponds the first-order $G^{+\bullet}$ deprotonation, from which the deprotonation rate constant k_D is obtained to be 2.1×10^5 s^{-1}. This value is close to the reported N_2-H deprotonation rate constant (3.5×10^5 s^{-1}),[28] corroborating further that the deprotonation site in G-quadruplex $AG_3(T_2AG_3)_3$ is N_2-H. In addition, the assignment of the absorption band at 640 nm (Figure 1B) to $G(N_2-H)^\bullet$ can be strengthened. According to this rate constant (2.1×10^5 s^{-1}), the deprotonation will complete within 5 μs in $AG_3(T_2AG_3)_3$. With such a slow deprotonation rate in the G-quadruplex, the transients $G^{+\bullet}$ prior to deprotonation can be accumulated and thus detected in the 1 μs spectra as shown in Figure 1B.

Here the deprotonation rate constant (2.1×10^5 s^{-1}) obtained for G-quadruplex $AG_3(T_2AG_3)_3$ is 20-fold smaller than that measured by pulse radiolysis (4.0×10^6 s^{-1}).[23] However, it is important to realize that the rates were obtained under different conditions. First, the method to generate the oxidizing radical $SO_4^{-\bullet}$ is different. In the pulse radiolysis experiment,[23] the hydrated electron (e_{aq}^-) was generated by electron beam irradiation and then reacted with $S_2O_8^{2-}$ to produce $SO_4^{-\bullet}$.[23] The generated e_{aq}^- may not only react with $S_2O_8^{2-}$ but also can interact directly with the G-quadruplex by attaching to the T base in the sequence most likely.[41] The deprotonation rate in G-quadruplex with or without a hydrated electron may be different. In our experiment, 355 nm photolysis of $S_2O_8^{2-}$ was used to produce $SO_4^{-\bullet}$. The 355 nm laser itself does not interact with G-quadruplex. This straightforward method thus makes sure that only $SO_4^{-\bullet}$ was produced to interact with G-quadruplex, avoiding other interference (e_{aq}^-) for the detection of the deprotonation after oxidation. Second, the deprotonation rate constant was obtained at pH 7.0 in our experiment, while the pH 7.4 was used by pulse radiolysis.[23] The higher pH will also lead to faster deprotonation rate. Although the obtained absolute values of the rate constants are different, the trend of the slower deprotonation rate in G-quadruplex compared to dsDNA was also mentioned in the pulse radiolysis experiments,[23] which is in general agreement with our observation.

Similar experiments were performed for G-quadruplexes $(G_4T_4G_4)2$ and $(TG_4T)4$. The transient absorption spectra (Figures S4A and S5A) obtained from the reaction of G-quadruplexes $(G_4T_4G_4)2/(TG_4T)4 + SO_4^{-\bullet}$ display similar features to that of G-quadruplex $AG_3(T_2AG_3)_3 + SO_4^{-\bullet}$, indicating that $G^{+\bullet}$ in G-quadruplexes $(G_4T_4G_4)2$ and $(TG_4T)4$ also undergoes deprotonation from N_2-H to form the neutral radical $G(N_2-H)^\bullet$. The rate constants obtained from the fast decay at 440 nm show similar linear dependence on the concentration of G-quadruplexes (as shown in Figures S4B and S5B), from which the bimolecular oxidation rate constants are obtained to be 2.2×10^9 and 2.1×10^9 M^{-1} s^{-1} for G-quadruplex $(G_4T_4G_4)2$ and $(TG_4T)4$, respectively. In addition, the rate constants obtained from the slower phase of 640 nm are independent of the G-quadruplex concentration (as shown in Figures S4B and S5B), yielding the rate constants for

DOI: 10.1021/ja510285t
J. Am. Chem. Soc. 2015, 137, 259−266

the $G^{+\bullet}$ deprotonation (2.0×10^5 and 1.8×10^5 s^{-1} for G-quadruplex $(G_4T_4G_4)2$ and $(TG_4T)4$, respectively), which are almost the same as the N_2−H deprotonation rate constant in $AG_3(T_2AG_3)_3$, confirming that the deprotonation site in $(G_4T_4G_4)2$ or $(TG_4T)4$ is also N_2−H.

Oxidation and Deprotonation of G-Quadruplex TBA. Although the DNA sequences which form G-quadruplexes $AG_3(T_2AG_3)_3$, $(G_4T_4G_4)2$ and $(TG_4T)4$ are different, each G base in these three sequences is hydrogen bonded to another two G bases to form G-quartet (Scheme 2), which may account for their similar spectral features and the same deprotonation site in these G-quadruplexes. However, if a non-hydrogen-bonded G base is introduced in the G-quadruplex, will the spectral signature and deprotonation site show a difference? In order to address this issue, the one-electron oxidation of G-quadruplex TBA, which has a monomer G in the loop (Scheme 2), was investigated.

Figure 2A shows the transient spectra of G-quadruplex TBA after oxidation by $SO_4^{-\bullet}$. Interestingly, the spectral feature

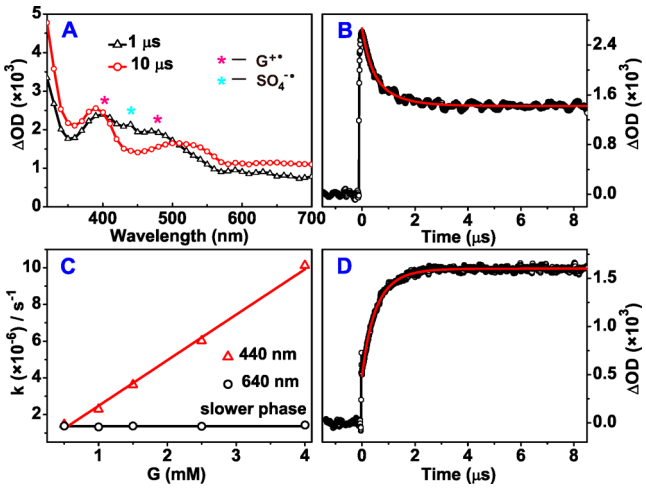

Figure 2. (A) Transient UV−vis spectra for buffer solution (pH = 7.0) of G-quadruplex TBA ([G] = 1.5 mM) + $K_2S_2O_8$ (120 mM) upon 355 nm laser flash photolysis. (B) Kinetics trace at 440 nm after excitation of (A) solution, with the single-exponential fit to the data (solid line). (C) Concentration dependence of rate constants obtained from the fast decay of 440 nm band (red triangle) and the slower phase increase of 640 nm band (black circle), respectively. (D) Kinetics trace at 640 nm after excitation of (A) solution, with the double-exponential fits to the data (solid line).

indicates that the deprotonation site in TBA is quite different from that in the other three G-quadruplexes, leading to the N_1−H deprotonated neutral radical $G(N_1-H)^\bullet$. As shown in Figure 2A, with the decay of 1 μs transients of $G^{+\bullet}$ at 400 and 480 nm and $SO_4^{-\bullet}$ at 440 nm, two resolved bands at 390 and 510 nm as well as flat absorption above 600 nm are observed in the 10 μs spectrum, which is the standard absorption pattern of $G(N_1-H)^\bullet$[19,28,29] and different from the characteristic 640 nm absorption peak for $G(N_2-H)^\bullet$ shown in Figure 1B.

As shown in Figure 2B, the $SO_4^{-\bullet}$ band at 440 nm contains a fast decay, corresponding to the chemical quenching of $SO_4^{-\bullet}$ by reaction with TBA. From the linear concentration dependence (Figure 2C), the bimolecular reaction rate constant to form $G^{+\bullet}$ is determined to be 2.5×10^9 M^{-1} s^{-1}. Further, by following the transient absorption above 600 nm, the deprotonation rate in G-quadruplex TBA can be determined because $G(N_1-H)^\bullet$ exhibits more intense absorbance from 600 to 700 nm than $G^{+\bullet}$.[29] As shown in Figure 2D, the growth of the band above 600 nm contains two components and fits well to a biexponential function with time constants of 331 and 694 ns, respectively. The fast time constant (331 ns) is in concomitant with the $SO_4^{-\bullet}$ decay at 440 nm (296 ns) (Figure 2B) and is corresponding to the oxidation to form $G^{+\bullet}$. The slower time constant (694 ns) is shown to be independent of concentration (Figure 2C), corresponding to the first-order deprotonation process to form the neutral radical $G(N_1-H)^\bullet$. The obtained deprotonation rate constant is 1.4×10^6 s^{-1}, much larger than the N_2−H deprotonation ($\sim 2.0 \times 10^5$ s^{-1}) in the other three G-quadruplexes. Together with the observed feature of $G(N_1-H)^\bullet$ in the transient spectra, these results suggest that deprotonation site in G-quadruplex TBA should mainly take place with the imino proton (N_1−H). As will be discussed later, there might be also some N_2−H deprotonation happening, which makes the deprotonation in TBA (1.4×10^6 s^{-1}) still slower than the case in free base dG (1.8×10^7 s^{-1}).[17]

Kinetic Isotope Effect. It shows in the above transient absorption experiments that the guanine cation radical in the G-quadruplexes $AG_3(T_2AG_3)_3$, $(G_4T_4G_4)2$, and $(TG_4T)4$ is subject to amino deprotonation (loss of the N_2−H), while the deprotonation occurs primarily with the imino N_1−H for TBA. The different deprotonation sites may be related to the G base surroundings. In G-quadruplex TBA, two types of G base exist: G base in the G-quartet and G base in the loop (Scheme 2). The N_1−H of G base in the G-quartet is hydrogen bonded (Scheme 1), while the N_1−H of G base in the loop is free. For $AG_3(T_2AG_3)_3$, $(G_4T_4G_4)2$, and $(TG_4T)4$, G bases only exist in the G-quartet surroundings, where N_1−H of G base is all hydrogen bonded, and one of the N_2−H atoms (H_{2a}) is hydrogen bonded while another is free (H_{2b}) (Scheme 1). According to previous results,[18] KIE on the deprotonation rate for the tightly bound (hydrogen bonded) proton and for the free proton is different. Therefore, we perform further KIE experiments to examine the deprotonation sites and its relationship with the H-bonding surroundings.

One-electron oxidation of the free base dG by $SO_4^{-\bullet}$ in H_2O and D_2O was measured first to obtain the KIE for the deprotonation of free proton. For the free base dG, both the bimolecular oxidation ($k_O = 7.2 \times 10^9$ M^{-1} s^{-1}) and the subsequent deprotonation ($k_D = 1.8 \times 10^7$ s^{-1}) occurs rapidly.[17] To discriminate the two fast processes individually, we adopted the same method as Kobayashi, determining the rate constant of deprotonation at dG concentrations above 3 mM when deprotonation is the rate-limiting step.[17] Figure 3 compares the absorbance change at 640 nm after photolysis of dG in H_2O and D_2O, from which the deprotonation rate constants of $G^{+\bullet}$ to $G(N_1-H)^\bullet$ are obtained ($k_{H_2O} = 1.9 \times 10^7$ s^{-1} and $k_{D_2O} = 1.2 \times 10^7$ s^{-1}). Thus, the KIE on the reaction rate is 1.6 for the free base dG, which is in agreement with the value of 1.7 obtained by Kobayashi.[18]

Similar KIE experiments were performed for the four G-quadruplexes, and the results are shown in Figure 4. As can be seen, the absorbance change at 640 nm consists of a fast and a slow growth, as discussed earlier, corresponding to the $G^{+\bullet}$ formation and deprotonation, respectively. It is first noticeable that the fast growth phase due to the $G^{+\bullet}$ formation is not significantly affected by H_2O or D_2O. In fact, the rate constant of $G^{+\bullet}$ formation, obtained either from the fast growth phase at 640 nm or the decay at 440 nm, shows no KIE due to the fact

DOI: 10.1021/ja510285t
J. Am. Chem. Soc. 2015, 137, 259−266

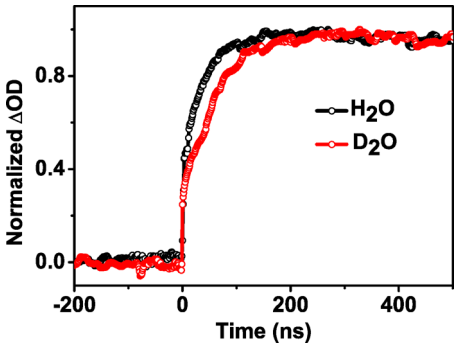

Figure 3. Normalized absorbance changes at 640 nm after 355 nm laser flash photolysis of $K_2S_2O_8$ (120 mM) and dG (5 mM) in 50 mM potassium phosphate buffer in H_2O at pH 7.0 (black) or in D_2O at pD 7.0 (red).

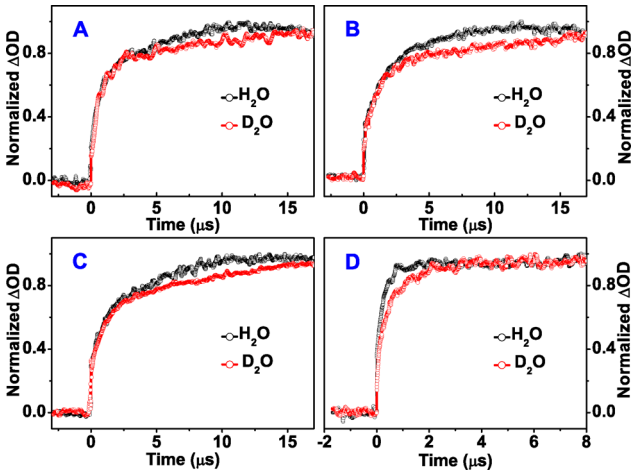

Figure 4. Normalized absorbance changes at 640 nm after 355 nm laser flash photolysis of $Na_2S_2O_8$ (120 mM) with quadruplexes $AG_3(T_2AG_3)_3$ ([G] = 1.5 mM, A) and $(G_4T_4G_4)2$ ([G] = 1.5 mM, B) or $K_2S_2O_8$ (120 mM) with quadruplexes $(TG_4T)4$ ([G] = 1.5 mM, C) and TBA ([G] = 1.5 mM, D) in 50 mM potassium or sodium phosphate buffer in H_2O at pH 7.0 (black) or in D_2O at pD 7.0 (red).

that H_2O is not involved in the one-electron oxidation process.[18] In contrast, for the 640 nm slow growth phase (deprotonation process), the rate in D_2O is markedly slower than that in H_2O, demonstrating obvious KIE. The deprotonation rate constants in H_2O or D_2O are determined (Table 1), making the KIE factors on the reaction rate to be 1.5, 1.8, 1.8, and 1.7 for G-quadruplexes $AG_3(T_2AG_3)_3$, $(G_4T_4G_4)2$, $(TG_4T)4$, and TBA, respectively (Table 1).

Table 1. Rate Constants of $G^{+\bullet}$ Formation (k_O) and Deprotonation (k_D) Determined at 440 and 640 nm, Respectively, in H_2O or D_2O[a]

G-quadruplex		$AG_3(T_2AG_3)_3$	$(G_4T_4G_4)_2$	$(TG_4T)_4$	TBA
H_2O	k_O[b]	2.1 ± 0.1	2.2 ± 0.1	2.1 ± 0.1	2.5 ± 0.1
	k_D[c]	2.1 ± 0.1	2.0 ± 0.1	1.8 ± 0.1	14 ± 1
D_2O	k_O[b]	2.0 ± 0.1	2.2 ± 0.1	2.2 ± 0.1	2.4 ± 0.1
	k_D[c]	1.4 ± 0.1	1.1 ± 0.1	1.0 ± 0.1	8.1 ± 0.1
KIE factor	k_O	1.0	1.0	1.0	1.0
	k_D	1.5	1.8	1.8	1.7

[a]KIE factors are also shown. [b]Unit is 10^9 M^{-1} s^{-1}. [c]Unit is 10^5 s^{-1}.

For $AG_3(T_2AG_3)_3$, $(G_4T_4G_4)2$, and $(TG_4T)4$, the KIE has values (1.5−1.8) comparable to the free base dG (1.6), indicating that the free proton (N_2−H_{2b}, Scheme 1) rather than the hydrogen-bonded proton (N_2−H_{2a} or N_1−H) is released during deprotonation. It is known that the deprotonation of the tightly bound proton should make the isotope effect to be about 3.8,[18] twice of the isotope effect of the free base dG. For TBA, the KIE value (1.7) is also comparable to that of the free base dG, indicating that the free N_1−H of G is responsible for the deprotonation. Because the N_1−H of G bases in G-quartet are all hydrogen bonded (Scheme 1) and that in the TGT loop is free, the loop G base should be responsible for the N_1−H deprotonation in TBA.

Deprotonation Mechanisms. For the free base dG after one-electron oxidation, $G^{+\bullet}$ deprotonates from N_1−H rather than N_2−H because N_1−H has the smaller pK_a value.[29] In G-quadruplexes $AG_3(T_2AG_3)_3$, $(G_4T_4G_4)2$, and $(TG_4T)4$, the deprotonation sites are N_2−H, different from that of the free base dG. The reason may be the special proton surroundings in G-quadruplexes. When a G base (red one, for example in Scheme 1) in G-quartet is oxidized to $G^{+\bullet}$, it may deprotonate from N_1−H or N_2−H, because these three protons are active. But N_1−H and N_2−H_{2a} are hydrogen bonded with O_6 and N_7 of another G base, respectively (shown in Scheme 1). In fact, the proton can be transferred from donor (deprotonation) site to acceptor (protonation) site only when the pK_a of donor (deprotonation) site is smaller than that of the acceptor (protonation) site. For the acceptor site, the protonation pK_a of G at N_7 is 2.4, and the pK_a for protonation at O_6 is expected to be even smaller than 2.4 as N_7 is the most readily protonated.[42] For the donor site, the deprotonation pK_a of $G^{+\bullet}$ from N_1−H or N_2−H is 3.9 and 4.7,[29] respectively. Therefore, the proton transfer from N_1−H of $G^{+\bullet}$ to O_6 of another G, or from N_2−H of $G^{+\bullet}$ to N_7 of another G, is thermodynamically infeasible in the G-quartet surroundings. On the other hand, the free proton N_2−H_{2b} in the G-quartet is exposed to the solvent, it can be released to the aqueous solvent directly to form $G(N_2-H)^{\bullet}$. According to the pK_a analysis, the deprotonation in G-quartet can only occur with the free proton N_2−H_{2b} when the hydrogen-bonded protons (N_1−H or N_2−H_{2a}) are not allowed to be transferred and released. It should be noticed that the situation in G-quartet is different from that in dsDNA. In dsDNA, the G base is paired with cytosine (C) through hydrogen bonding (Scheme 1). When $G^{+\bullet}$ is formed in dsDNA, the effect of base pairing is to transfer the N_1 proton of $G^{+\bullet}$ to N_3 of C in the base pair, after which the N_1 proton is eventually released into solvent, as the protonation pK_a of N_3 in C (4.3) is slightly higher than the deprotonation pK_a of N_1 in $G^{+\bullet}$ (3.9).[17,18] This makes the N_1−H deprotonation feasible in dsDNA.[17,18]

In G-quadruplexes $AG_3(T_2AG_3)_3$, $(G_4T_4G_4)2$ or $(TG_4T)4$, each G base is hydrogen bonded to another two G bases to form G-quartet (Scheme 2). According to the pK_a analysis above, it is impossible to deprotonate from the hydrogen-bonded N_1−H or N_2−H_{2a} in G-quartet. The $G^{+\bullet}$ formed in these three G-quadruplexes would deprotonate only from the free proton N_2−H_{2b} leading to $G(N_2-H)^{\bullet}$ as initial product. Nevertheless, two types of G base exist in G-quadruplex TBA (Scheme 2). Both the loop G and G-quartet G are subject to oxidation to produce holes, and the positive charge is in equilibrium between the loop G and G-quartet.[43,44] When the hole locates at the G-quartet G base, $G^{+\bullet}$ would deprotonate from N_2−H_{2b}. Otherwise, when the hole locates at the loop G

DOI: 10.1021/ja510285t
J. Am. Chem. Soc. 2015, 137, 259−266

base, the situation is similar to the free base dG and the deprotonation site is N_1−H. Because the deprotonation rate constant of $G^{+\bullet}$ from N_1−H is much larger than that from N_2−H,[17,28] the N_1−H deprotonation of the loop $G^{+\bullet}$ should be predominant, while the N_2−H deprotonation in the G-quartet may co-exist to some extent. Thus, the transient spectra of TBA (Figure 2A) mainly display the feature of the N_1−H deprotonation product $G(N_1-H)^{\bullet}$. Meanwhile, because of the co-existence of the N_1−H and N_2−H deprotonation in G-quadruplex TBA, the rate constant is observed to be between the N_1−H deprotonation rate constant in free base dG[17] and the N_2−H deprotonation rate constant in the other three G-quadruplexes.

Comparison between G-Quadruplex and dsDNA. To compare the deprotonation rate constant of G-quadruplex DNA with that of dsDNA, comparative experiments were performed for the dsDNA formed by $AG_3(T_2AG_3)_3$ with its complementary strand. The deprotonation site in dsDNA is known to be N_1−H, with spectra obtained essentially similar to that of free dG.[17,18] Indeed, the transient spectra for $SO_4^{-\bullet}$ oxidizing the dsDNA of $AG_3(T_2AG_3)_3$ sequence (Figure 5A)

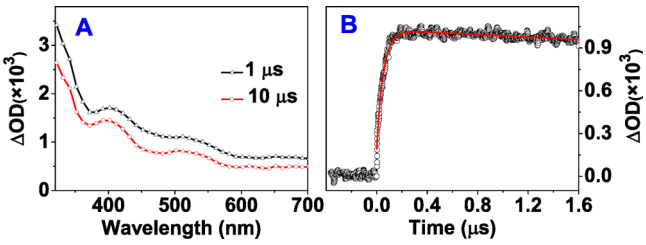

Figure 5. (A) Transient UV−vis spectra for buffer solution (pH = 7.0) of dsDNA ([G] = 1.5 mM) + $Na_2S_2O_8$ (120 mM) upon 355 nm laser flash photolysis. (B) Kinetics trace at 640 nm after excitation of buffer solution (pH = 7.0) of dsDNA ([G] = 6 mM) + $K_2S_2O_8$ (120 mM), with the first-order fit to the data (solid line).

corroborate the N_1−H deprotonation site, as manifested by the characteristic absorption pattern of $G(N_1-H)^{\bullet}$[19,28,29] with two absorption bands at 400 and 510 nm as well as flat absorption above 600 nm. To obtain the deprotonation rate constant, the absorbance change at 640 nm is measured at high dsDNA concentration ([G] = 6 mM) when the oxidation completes within ~30 ns, and deprotonation is the rate-limiting step. As shown in Figure 5B, the absorbance increase observed at 640 nm can be well fitted by a single-exponential function, yielding the deprotonation rate constant of 1.9×10^7 s^{-1}. This value is consistent with that obtained for other similar dsDNA sequences (2.0×10^7 s^{-1}).[18]

It is well accepted that the species responsible for the fast hole transfer along DNA is the cation radical $G^{+\bullet}$. Because $G^{+\bullet}$ is also subject to deprotonation forming neutral radicals, the hole transfer would be interrupted by deprotonation. Here, our experiments show that the deprotonation rate constant in G-quadruplex DNA (1.8×10^5 to 1.4×10^6 s^{-1}) is 1−2 orders of magnitude smaller than that in dsDNA (around 1.9×10^7 s^{-1}), indicating that the hole transfer tends to be less interrupted by deprotonation and thus the hole transfer distance could be longer with G-quadruplex DNA compared to dsDNA. In this regards, the G-quadruplex DNA can be a potentially better candidate for the design of DNA-based nanocircuitry. Additionally, it shows here that deprotonation occurs with a larger rate constant in G-quadruplexes with free G base in the loop (TBA) than the G-quadruplexes with all G bases hydrogen bonded in G-quartet ($AG_3(T_2AG_3)_3$, $(G_4T_4G_4)2$, and $(TG_4T)4$). This suggests further that in the design of G-quadruplex structure as molecular electronic devices, the free G base existing in the loop should be avoided.

When incorporated into molecular electronic devices, G-quadruplex can serve as a bridge between two gold electrodes[45] or single-walled carbon nanotube[21] through covalent bonding. The slow deprotonation rate is beneficial to retain the high conductance of G-quadruplexes for such applications. Also importantly, the lower ionization potential of G-quartet may facilitate DNA charge transfer that is known to occur through diffusive charge-hopping among low-energy G sites,[14−16] e.g. when conjugated with duplex DNA[20] such as $(A-T)_n$ sequence. Together with their slower deprotonation rate, G-quadruplexes could be a promising charge transfer unit.

CONCLUSION

In this work, we have studied the deprotonation process of $G^{+\bullet}$ in G-quadruplexes after one-electron oxidation by nanosecond laser flash photolysis spectroscopy. Unusual deprotonation behaviors are observed. Different from the imino proton (N_1−H) loss in free base dG and dsDNA, for G-quadruplex $AG_3(T_2AG_3)_3$, $(G_4T_4G_4)2$, and $(TG_4T)4$, it is found that the amino proton (N_2−H) is deprotonated, forming the $G(N_2-H)^{\bullet}$ radical with characteristic transient absorption peak at 640 nm. For G-quadruplex TBA, deprotonation occurs mainly with the imino proton (N_1−H) leading to $G(N_1-H)^{\bullet}$ as the neutral product. The deprotonation rate constants obtained are 2.1×10^5, 2.0×10^5, 1.8×10^5, and 1.4×10^6 s^{-1}, respectively, for $AG_3(T_2AG_3)_3$, $(G_4T_4G_4)2$, $(TG_4T)4$, and TBA, confirming the deprotonation site for the four G-quadruplexes. Further kinetic isotope measurements and pK_a analysis suggest that it should be the non-hydrogen-bonded free proton to be released during deprotonation in G-quadruplexes, which is the free N_2−H exposed to solvent for G bases in G-quartets or the free N_1−H for G base in the loop. For $AG_3(T_2AG_3)_3$, $(G_4T_4G_4)2$, and $(TG_4T)4$ that has all G bases hydrogen bonded in G-quartets, the deprotonation can only occur with the free proton N_2−H_{2b} in G-quartet, whereas for G-quadruplex TBA that has a free G base in the loop, the $G^{+\bullet}$ in the loop is prone to deprotonation due to the faster N_1−H deprotonation rate, leading to the predominance of N_1−H deprotonation of the loop $G^{+\bullet}$ over the slower N_2−H deprotonation in the G-quartet for TBA.

Overall, it is shown that the deprotonation rate constants in four G-quadruplexes are 1−2 orders of magnitude smaller than that in dsDNA (1.9×10^7 s^{-1}). Due to the competition between charge transfer and the deprotonation of $G^{+\bullet}$, the slower deprotonation rates in G-quadruplex DNA are expected to result in less interruption of hole transfer and therefore longer distance of hole transfer with G-quadruplex DNA compared to dsDNA. The unique deprotonation features observed here for G-quadruplexes open possibilities for their interesting applications as molecular electronic devices. Moreover, the elucidated mechanisms can provide illuminations for the rational design of G-quadruplex structures toward such applications, indicating that the G-quadruplex structure without G base in the loop is more ideal because the G base in the loop will cause faster deprotonation.

DOI: 10.1021/ja510285t
J. Am. Chem. Soc. 2015, 137, 259−266

■ ASSOCIATED CONTENT

Supporting Information

$SO_4^{-\bullet}$ spectra, CD spectra, and additional transient absorption data. This material is available free of charge via the Internet at http://pubs.acs.org.

■ AUTHOR INFORMATION

Corresponding Author

hongmei@iccas.ac.cn

Author Contributions

‡These authors contributed equally.

Notes

The authors declare no competing financial interest.

■ ACKNOWLEDGMENTS

This work was financially supported by the National Natural Science Foundation of China (grant nos. 21333012 and 21425313), the National Basic Research Program of China (2013CB834602), and the Chinese Academy of Sciences (Project XDB12020200).

■ REFERENCES

(1) Endres, R. G.; Cox, D. L.; Singh, R. R. P. *Rev. Mod. Phys.* **2004**, *76*, 195−214.
(2) Malyshev, A. V. *Phys. Rev. Lett.* **2007**, *98*, 96801−96804.
(3) Nogues, C.; Cohen, S. R.; Daube, S.; Apter, N.; Naaman, R. *J. Phys. Chem. B* **2006**, *110*, 8910−8913.
(4) Giese, B. *Acc. Chem. Res.* **2000**, *33*, 631−636.
(5) Schuster, G. B. *Acc. Chem. Res.* **2000**, *33*, 253−260.
(6) Takada, T.; Kawai, K.; Fujitsuka, M.; Majima, T. *Proc. Natl. Acad. Sci. U.S.A.* **2004**, *101*, 14002−14006.
(7) Lewis, F. D.; Liu, J. Q.; Zuo, X. B.; Hayes, R. T.; Wasielewski, M. R. *J. Am. Chem. Soc.* **2003**, *125*, 4850−4861.
(8) Lewis, F. D.; Liu, X. Y.; Liu, J. Q.; Miller, S. E.; Hayes, R. T.; Wasielewski, M. R. *Nature* **2000**, *406*, 51−53.
(9) Pittman, T. L.; Miao, W. *J. Phys. Chem. C* **2008**, *112*, 16999−17004.
(10) Storhoff, J. J.; Mirkin, C. A. *Chem. Rev.* **1999**, *99*, 1849−1862.
(11) Seeman, N. C. *Angew. Chem., Int. Ed.* **1998**, *37*, 3220−3238.
(12) Seidel, C. A. M.; Schulz, A.; Sauer, M. H. M. *J. Phys. Chem.* **1996**, *100*, 5541−5553.
(13) Steenken, S.; Jovanovic, S. V. *J. Am. Chem. Soc.* **1997**, *119*, 617−618.
(14) Meggers, E.; Michel-Beyerle, M. E.; Giese, B. *J. Am. Chem. Soc.* **1998**, *120*, 12950−12955.
(15) Nakatani, K.; Dohno, C.; Saito, I. *J. Am. Chem. Soc.* **1999**, *121*, 10854−10855.
(16) Osakada, Y.; Kawai, K.; Fujitsuka, M.; Majima, T. *Proc. Natl. Acad. Sci. U.S.A.* **2006**, *103*, 18072−18076.
(17) Kobayashi, K.; Tagawa, S. *J. Am. Chem. Soc.* **2003**, *125*, 10213−10218.
(18) Kobayashi, K.; Yamagami, R.; Tagawa, S. *J. Phys. Chem. B* **2008**, *112*, 10752−10757.
(19) Rokhlenko, Y.; Geacintov, N. E.; Shafirovich, V. *J. Am. Chem. Soc.* **2012**, *134*, 4955−4962.
(20) Delaney, S.; Barton, J. K. *Biochemistry* **2003**, *42*, 14159−14165.
(21) Liu, S.; Zhang, X. Y.; Luo, W. X.; Wang, Z. X.; Guo, X. F.; Steigerwald, M. L.; Fang, X. H. *Angew. Chem., Int. Ed.* **2011**, *50*, 2496−2502.
(22) Woiczikowski, P. B.; Kubar, T.; Gutierrez, R.; Cuniberti, G.; Elstner, M. *J. Chem. Phys.* **2010**, *133*, 35103−35114.
(23) Choi, J.; Park, J.; Tanaka, A.; Park, M. J.; Jang, Y. J.; Fujitsuka, M.; Kim, S. K.; Majima, T. *Angew. Chem., Int. Ed.* **2013**, *52*, 1134−1138.
(24) Rottger, K.; Schwalb, N. K.; Temps, F. J. *Phys. Chem. A* **2013**, *117*, 2469−2478.
(25) Changenet-Barret, P.; Hua, Y.; Markovitsi, D. Electronic Excitations in Guanine Quadruplexes. *In Topics in Current Chemistry*; Springer: Berlin Heidelberg, 2014.
(26) Wellinger, R. J.; Sen, D. *Eur. J. Cancer* **1997**, *33*, 735−749.
(27) Davis, J. T. *Angew. Chem., Int. Ed.* **2004**, *43*, 668−698.
(28) Candeias, L.; Steenken, S. *J. Am. Chem. Soc.* **1992**, *114*, 699−704.
(29) Candeias, L.; Steenken, S. *J. Am. Chem. Soc.* **1989**, *111*, 1094−1099.
(30) Cantor, C. R.; Warshaw, M. M.; Shapiro, H. *Biopolymers* **1970**, *9*, 1059−1077.
(31) Mcelroy, W. J. *J. Phys. Chem.* **1990**, *94*, 2435−2441.
(32) Wang, Y.; Patel, D. J. *Structure* **1993**, *1*, 263−282.
(33) Fleming, A. M.; Burrows, C. *J. Chem. Res. Toxicol.* **2013**, *26*, 593−607.
(34) Smith, F. W.; Feigon, J. *Nature* **1992**, *356*, 164−168.
(35) Ida, R.; Wu, G. *J. Am. Chem. Soc.* **2008**, *130*, 3590−3602.
(36) Aboulela, F.; Murchie, A. I. H.; Norman, D. G.; Lilley, D. M. J. *J. Mol. Biol.* **1994**, *243*, 458−471.
(37) Macaya, R. F.; Schultze, P.; Smith, F. W.; Roe, J. A.; Feigon, J. *Proc. Natl. Acad. Sci. U.S.A.* **1993**, *90*, 3745−3749.
(38) Candeias, L. P.; Steenken, S. *Chem.—Eur. J.* **2000**, *6*, 475−484.
(39) Chatgilialoglu, C.; D'Angelantonio, M.; Guerra, M.; Kaloudis, P.; Mulazzani, Q. G. *Angew. Chem., Int. Ed.* **2009**, *48*, 2214−2217.
(40) Chatgilialoglu, C.; Caminal, C.; Guerra, M.; Mulazzani, Q. G. *Angew. Chem., Int. Ed.* **2005**, *44*, 6030−6032.
(41) Yamagami, R.; Kobayashi, K.; Tagawa, S. *Chem.—Eur. J.* **2009**, *15*, 12201−12203.
(42) Parker, A. W.; Lin, C. Y.; George, M. W.; Towrie, M.; Kuimova, M. K. *J. Phys. Chem. B* **2010**, *114*, 3660−3667.
(43) Ndlebe, T.; Schuster, G. B. *Org. Biomol. Chem.* **2006**, *4*, 4015−4021.
(44) Huang, Y. C.; Cheng, A. K. H.; Yu, H. Z.; Sen, D. *Biochemistry* **2009**, *48*, 6794−6804.
(45) Liu, S. P.; Weisbrod, S. H.; Tang, Z.; Marx, A.; Scheer, E.; Erbe, A. *Angew. Chem., Int. Ed.* **2010**, *49*, 3313−3316.

DOI: 10.1021/ja510285t
J. Am. Chem. Soc. 2015, 137, 259−266